

Dear Editors and Reviewers,

Thank you very much for your careful review and helpful comments on our manuscript acp-2020-708. We appreciate very much your constructive comments and suggestions on our manuscript. We have accordingly made the careful and substantial revisions. The revised portions are highlighted in the revised manuscript. Please find our point to point responses to the reviewer's comments as follows:

## **Responses to the reviewer 2**

*[The authors have carried out MV-EOF and EEOF analysis to select and understand the peak pollution episodes and corresponding pollution pathways and meteorological conditions during these events using data from 2015 to 2019 over the middle Yangtze River area in China. In addition, they have also carried our chemistry-climate model simulations to understand the same issue but for a typical event for corroboration.*

*Though I would like to appreciate the overall effort and the intention of the authors, I found it hard to follow the manuscript due to the following reasons.]*

**Response 1:** Thank the referee very much for the careful review and encouraging comments on our manuscript. We have accordingly made the careful revisions. The revised portions are highlighted in the revised manuscript. In the following we quoted each review question in the square brackets and added our response after each paragraph.

*[The weakest part of the paper is the data and methodology section where scant information is provided with regard to the data, its curation and analysis including the details about numerical simulations.*

*The whole paper depends on the analysis of PM<sub>2.5</sub> pollution based on data from the China's National Ambient Air Quality Monitoring Network. Even basic information about this dataset is missing in the manuscript. For example, it is not clear whether this is a gridded data or station data? What is the temporal resolution? What is the spatial resolution of the chemistry-climate model simulations? ]*

**Response 2:** In response to the referee's comments, we have reorganized and modified the data and methodology section as follows:

## **2 Data and methods**

### **2.1 Observational data**

In this study, the daily average PM<sub>2.5</sub> concentrations in January over 2015-2019 are obtained from more than 1600 air quality monitoring stations in China (<http://datacenter.mee.gov.cn/>) to display the spatial distribution of PM<sub>2.5</sub> in central and eastern China. The air quality observation data are through quality control based on China's national standard of air quality observation. The PM<sub>2.5</sub> concentrations observed at 31 major cities in Hubei and Hunan provinces are selected to represent the air pollution levels in the Twain-Hu Basin (Fig. 1c) to construct the joint observation matrix of MV-EOF decomposition in the THB.

The meteorological observation data in January 2015-2019 are downloaded from the hourly surface data from the China Meteorological Science Data Center (<http://data.cma.cn/>). In this study, meteorological observations including sea level pressure (SLP), 2-m air temperature, 10-m wind speed and wind direction, are also used to construct the joint observation matrix of the MV-EOF decomposition of the THB,

The radiosonde observations of air temperature and wind speed from Wuhan and Changsha meteorological stations (Fig. 1c) are adopted as well to analyze the atmospheric thermodynamic vertical structures during wintertime and regional PM<sub>2.5</sub> transport cases in the THB in the recent 5 years.

In addition, in order to analyze the synoptic circulation pattern and atmospheric thermodynamic vertical structure during the wintertime air pollution in the THB with regional PM<sub>2.5</sub> transport, we use the ERA-interim daily reanalysis data with 0.25°×0.25° resolution (<https://apps.ecmwf.int/datasets/data/interim-full-daily/>), which consists the atmospheric boundary layer height, SLP, 2-m temperature, 10-m wind vector components u and v, as well as the geopotential height, air temperature, vertical speed, and wind vector components u and v at different vertical layers in January 2015-2019.

## 2.2 Decomposition of multivariable empirical orthogonal function (MV-EOF)

The empirical orthogonal function (EOF) analysis is a method used to identify patterns of simultaneous variation (Schepanski et al., 2016). The EOF can concentrate the information of original field into several main modes to describe the changes of the complex element field through the dimensionality reduction. The principle is to decompose the spatio-temporal matrix of observation data into a linear combination of the spatial eigenvector matrix and the corresponding time coefficient matrix.

The observation data of a certain variable field is given in the form of  $X_{mn}$  matrix:

$$X = \begin{bmatrix} X_{11} & \cdots & X_{1n} \\ \vdots & & \\ X_{m1} & \cdots & X_{mn} \end{bmatrix} \quad (1)$$

where  $m$  is the space point (it can be the number of stations or grid points),  $n$  is the length of time series. Through EOF expansion, Formula (1) is decomposed into the product of the space function  $V$  and the time function  $T$ , and the matrix form is

$$X = VT \quad (2)$$

where:

$$V = \begin{bmatrix} v_{11} & \cdots & v_{1m} \\ \vdots & & \\ v_{m1} & \cdots & v_{mm} \end{bmatrix}, \quad T = \begin{bmatrix} t_{11} & \cdots & t_{1n} \\ \vdots & & \\ t_{m1} & \cdots & t_{mn} \end{bmatrix} \quad (3)$$

$V$  is called the spatial function matrix (space mode), which represents a typical field that does not change with time;  $T$  is called the time coefficient matrix, representing the weight coefficient of the spatial mode.

We process  $X_{mn}$  as an anomaly, get the eigenroot  $\lambda_m$  and eigenvector  $v_m$  of the real symmetric matrix, and then calculate the variance contribution rate  $\rho_i$  of the  $i$ -th eigenvector and the cumulative variance contribution rate  $P_i$  of the first  $p$  eigenvectors:

$$\rho_i = \lambda_i / \sum_{i=1}^m \lambda_i \quad (4)$$

$$P_i = \frac{\sum_{i=1}^p \lambda_i}{\sum_{i=1}^m \lambda_i} \quad (5)$$

The eigenvector represents the variation structure of a variable field, and its spatial distribution form the main distribution structure of variable field. The corresponding time coefficient is positive, indicating that the variable at that time has the same variation trend as this type of distribution. On the contrary, a negative coefficient denotes that the changing trend of variable at the corresponding time is opposite to this kind of distribution, and larger value means a more significant corresponding spatial distribution.

The multivariate empirical orthogonal function (MV-EOF) decomposition is an extended variant of EOF (Wang et al., 1992; 2008). In this method, two or more variables with the same time length and space points are standardized, and a new variable field is constructed, and then EOF decomposition is performed on the new variables. MV-EOF has advantages in simultaneously representing the spatial distributions of multiple elements and the spatial connections among various elements, and can be used to explore the coupling process of interactions in complex systems (Sparnocchia et al., 2003).

To obtain the synergistic variation of PM<sub>2.5</sub> concentration and meteorological elements in atmospheric circulations of heavy pollution events in the THB, we choose the daily average PM<sub>2.5</sub> concentrations, 10-m wind speed (including meridional and zonal components) and SLP from 31 urban observation sites in the THB in January of 2015-2019 for MV-EOF decomposition. Since the magnitude of different elements varies greatly, all elements have been standardized before the MV-EOF decomposition.

The data matrix  $X_{mn}$  constructed by using the four elements is as follows:

$$X_{mn} = [X_{m_1n}, X_{m_2n}, X_{m_3n}, X_{m_4n}] \quad (6)$$

where  $X_{m_1n}$ ,  $X_{m_2n}$ ,  $X_{m_3n}$  and  $X_{m_4n}$  represent PM<sub>2.5</sub>, SLP, 10-m meridional wind and zonal wind, respectively;  $m_1 = m_2 = m_3 = m_4 = 31$  is the number of urban observation sites in the THB,  $n = 155$  is the length of the daily time series in January of 2015-2019;

$X_{mn}$  is the extended new variable fields. Then, the new variable matrix is introduced into Formula (2) to do the EOF decomposition.

*[Since the objective of the paper is to study the peak pollution episodes during the five year period during the winter/January, which mode of the EOF was used finally used to create the several figures in the results section?*

*Was the climatology of the five-year period removed during the analysis? If not, the first mode will show up the climatological mean as the dominant feature.*

*Line 184 to 186 states about some synthetic and correlation analysis including anomalies. Was this the base database used for further EOF analysis?]*

**Response 3:** First three modes of the MV-EOF were used finally used to create the several figures in the results section, and the climatology of the five-year period was removed during the analysis with MV-EOF. In response to the referee's comments, we have reorganized and modified Section 3 as follows:

### **3. Results of MV-EOF decomposition and selection of typical air pollution events with regional transport**

#### **3.1 Analysis of MV-EOF decomposition**

Figure 2 shows the first three modes and their time series obtained by MV-EOF decomposition based on PM<sub>2.5</sub> concentration, 10-m wind speed (including meridional wind and zonal wind) and SLP at 31 observation sites in the THB in January of 2015-2019. The variance contribution rates of the three modes are 28.2%, 16.0%, and 12.0%, respectively, and the cumulative variance reaches 56.2%, all of which have passed the North test, indicating that the first three modes are independent of each other and can be clearly distinguished from other modes.

The spatial distributions of first three modes decomposed by MV-EOF could characterize the synergistic change of PM<sub>2.5</sub> concentrations with near-surface wind and

air pressure fields over the THB (Fig. 2). The first mode of positive  $PM_{2.5}$  loads distribution corresponded to the negative air pressure loads and weak wind loads (Fig. 2a), and the second and third modes of positive  $PM_{2.5}$  loads were distributed with the positive air pressure loads but with strong southerly and northerly wind loads (Figs. 2b-2c), reflecting the connections of regional  $PM_{2.5}$  pollution over the THB with low air pressure and weak winds (Fig. 2a), with high air pressure centered over the THB and strong southerly winds (Fig. 2b), and with high air pressure in northern THB strong northerly winds driving the transport of air pollutants from North China to the THB (Fig. 2c). The significantly larger  $PM_{2.5}$  loads in third mode comparing to the first and second modes (Figs. 2a, 2b and 2c) could imply an importance of regional  $PM_{2.5}$  transport in air pollution in the THB.

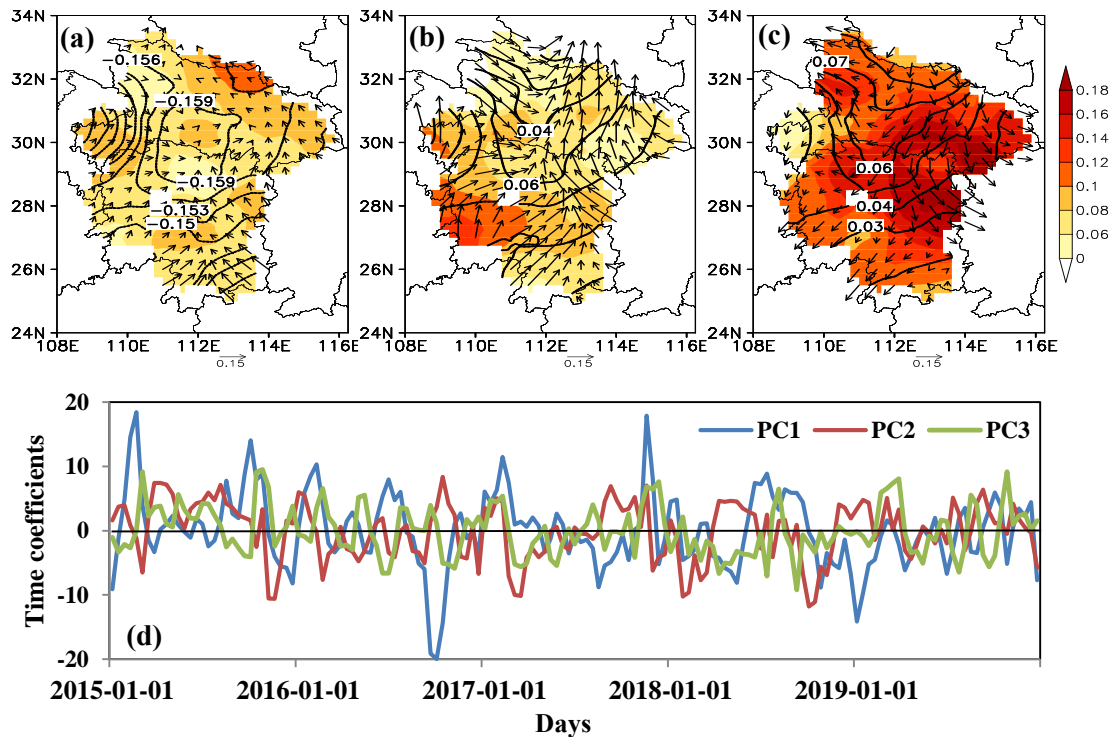


**Figure 2.** (a) The first mode, (b) the second mode and (c) the third mode decomposed by MV-EOF with  $PM_{2.5}$  loads (color contours), the SLP loads (black contour lines) and 10-m wind loads (vectors) as well as (d) the time coefficients PC1, PC2, and PC3 of the first three modes in January over 2015-2019.

The positive and negative time coefficients in the daily time series (Fig. 2d) showed the abnormally high and low PM<sub>2.5</sub> concentrations over the THB with meteorological influences on poor and good air quality. By , the third-mode time coefficients explained 48% of the total variance of the average PM<sub>2.5</sub> time variation in the THB (Fig. 3), which reflected an important role of regional PM<sub>2.5</sub> transport in increasing PM<sub>2.5</sub> in the THB.

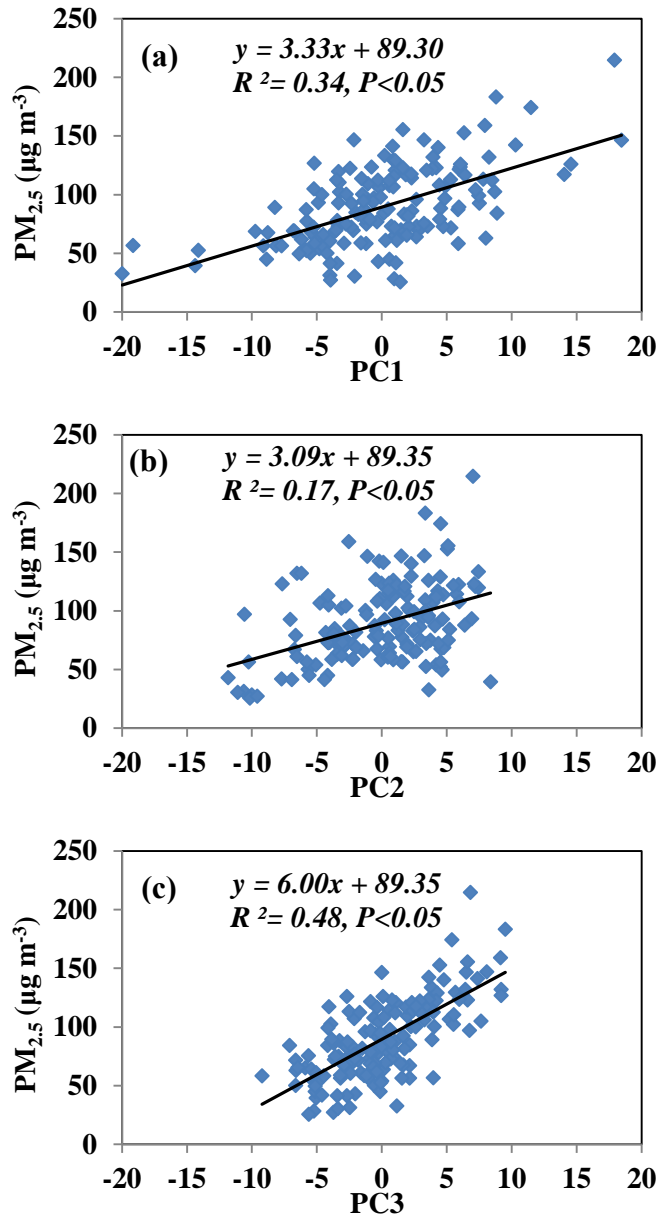


**Figure 3.** Scatter plots of (a) The first mode, (b) the second mode and (c) the third mode time coefficients PC1, PC2, and PC3 respectively with the daily PM<sub>2.5</sub> concentrations averaged over the THB in January of 2015-2019.

In order to explore the synoptic circulations on heavy air pollution in the THB, we correlated the daily changes of the time coefficients of the three modes (Fig. 2d) and 850hPa geopotential heights, vertical velocity and wind of the ERA-Interim daily data over January of 2015-2019 in CEC (Fig. 4). As seen from Figure 4, the correlation coefficients between the first-mode time coefficients of THB' decomposed  $PM_{2.5}$  and the 850-hPa heights were negative over the CEC, indicating that the anomalously high (low)  $PM_{2.5}$  concentrations corresponded to the abnormally low (high) 850-hPa height field (Fig. 4a). The low (high) pressure center in the northwestern region of THB was conducive to the accumulation (removal) of surface  $PM_{2.5}$  in the THB (Fig. 4a). The southerly winds block the vertical diffusion of pollutants, prone to local air pollutant accumulation and chemical transformation, which was similar to the heavy pollution in the Sichuan Basin of southwest China induced by the low-value system of the Southwest Vortex (Ning et al., 2018).

The correlation coefficients between the second-mode time coefficients and the 850-hPa height field were positive (Fig. 4b), suggesting that the heavy pollution in the THB was controlled with the high-pressure system with the obvious anticyclonic circulation and the significant downdrafts (the correlation coefficient of 850-hPa vertical velocity field is positive) at 850-hPa (Fig. 4b), which inhibited the vertical spread of air pollutants, strengthening the cumulative air pollution in the near-surface layer. This mechanism was also reported as a typical synoptic circulation for heavy  $PM_{2.5}$  pollution in central China (Yan et al., 2021).

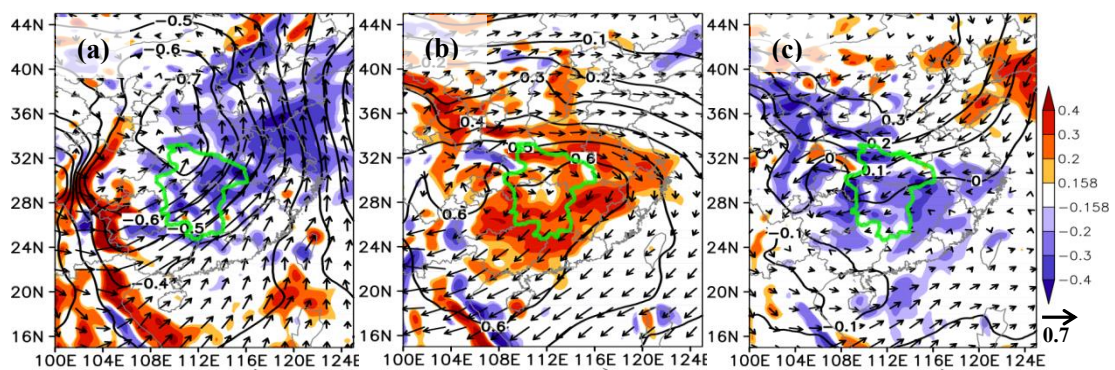


**Figure 4.** Spatial distribution of correlations of the time coefficients of (a) first mode, (b) second mode and (c) third mode respectively with the 850-hPa geopotential height



(black contour lines), vertical velocity (color contours) and winds (vectors) in January of 2015-2019. The critical correlation coefficient at the 95% significance test is 0.158.

In the third mode, the heavy pollution in the THB is controlled by the bottom of the high pressure over CEC (Fig. 4c and Fig. 5), and the obvious northeasterly airflows at 850 hPa (Fig. 4c) as well as the upraised boundary layer, and near-surface anomalous northerly winds (Fig. 5), which was a typical pattern of synoptic circulation for regional transport of PM<sub>2.5</sub> over north to central China (Yu et al. 2020). This circulation condition could drive air pollutants from the source areas of North China to the downwind THB. The meteorological mechanism of regional transport of air pollutants was studied in the following sections.

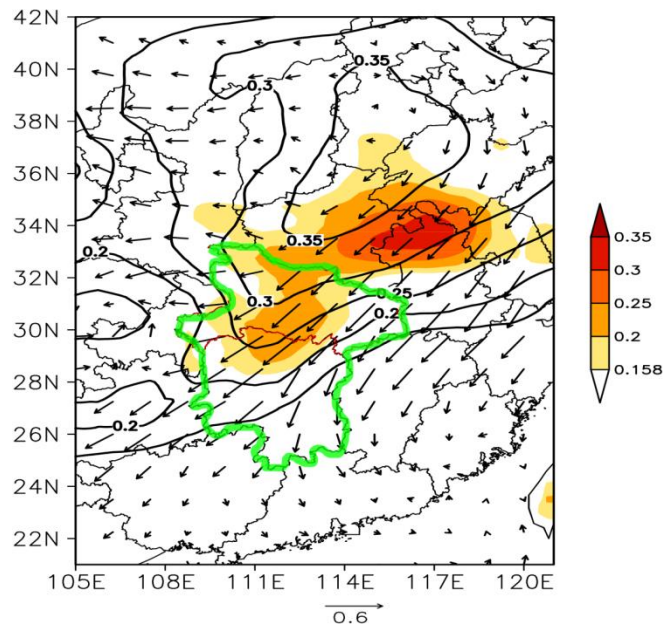


**Figure 5.** Spatial distribution of correlations of daily changes of the third-mode time coefficients respectively with the SLP (black contour lines), atmospheric boundary layer height (color contours) and 10-m wind vectors in January of 2015-2019. The critical correlation coefficient at the 95% significance test is 0.158, and the THB is roughly outlined with green lines.

*[Though the authors use several datasets and tools from the surface, reanalysis, and model simulations, the lack of information above basic aspects does not allow me to be positive. As such, in the current form, this manuscript requires substantial revision in terms of its readability and usefulness for a wide range of audiences of this journal. Hence I recommend rejection of the manuscript.]*

**Response 4:** Following the referee’s comments, we have made the substantial revisions with adding the information of data and methods including description of meteorological and environmental data as well as the introduction of decomposition of multi-variable empirical orthogonal function (MV-EOF) in terms of its readability and usefulness for a wide range of audiences of this journal.

*Minor Comments:*

*[1. Line 62 to 66, The sentence may be shortened.]*

**Response 5:** In the revised manuscript, we have shortened the sentence as follows: “Regional transport of air pollutants is an important issue in atmospheric environmental prevention (Wu et al., 2013b; Owen et al., 2006; Miao et al., 2017; Kozáková et al., 2019; Lu et al., 2019a).”

*[2. Line 73, in in is repeated.]*

**Response 6:** one “in” has been removed.

*[3. Line 76, What is meant by excessive anthropogenic emissions? Is there any specific emission relevant only for winter that does not exist during other periods?]*

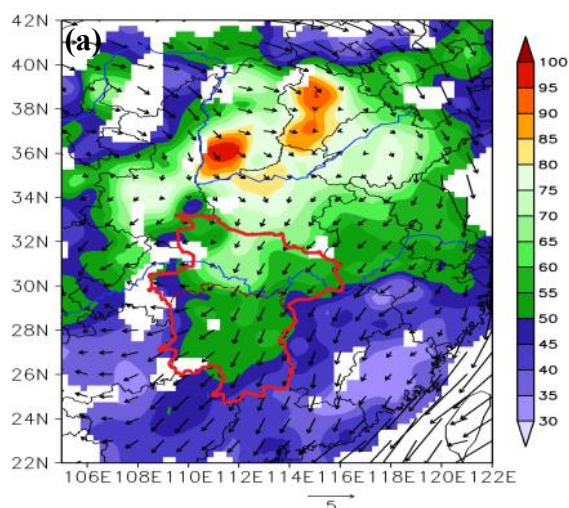
**Response 7:** We have deleted the sentence with “excessive emissions of air pollution” to avoid the misleading.

*[4. Most sentences are excessively long to understand. An English correction may help improve the readability of the manuscript.]*

**Response 8:** With the help of English Language editing service, the English witting errors including incorrect grammar, confusing wording and inappropriate expression have been substantially revised to improve the readability of the manuscript.

*[5. The authors need to explain where the study region is using a map. The area shown in the map is a huge region over China spread over tens of degrees across. It will be better to name the regions in a map for the reader’s benefit.]*

**Response 9:** Thank for the referee’s suggestion. We have accordingly outlined the study area:



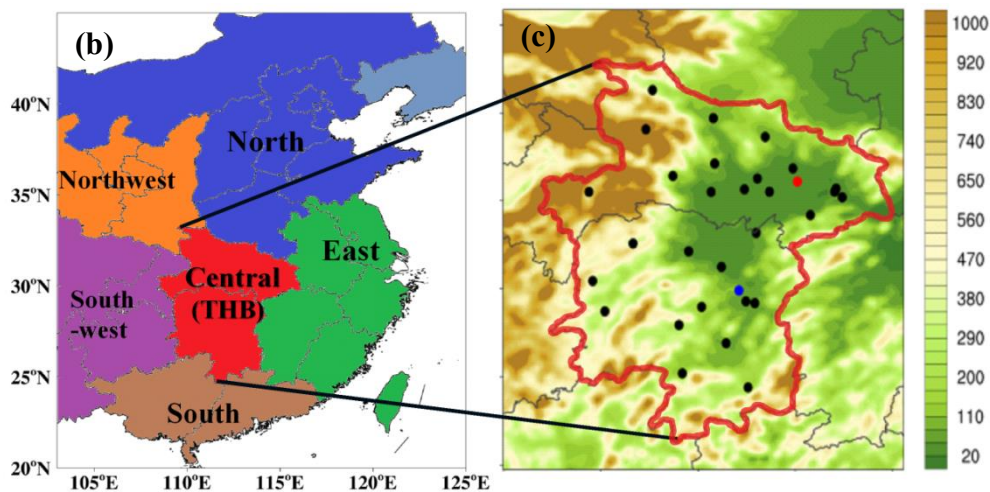


**Figure 1.** (a) The distribution of surface PM<sub>2.5</sub> concentrations (color contours, unit:  $\mu\text{g m}^{-3}$ ) and 10-m wind field (vectors, unit:  $\text{m s}^{-1}$ ) in CEC averaged during January of 2015-2019, (b) the geographical regions of China, and (c) the geographical distribution of 31 observation sites (dots) in the THB outlined with the red line, and the color contours representing the terrain height above sea level (unit: m), the red dot for Wuhan Station, and the blue dot for Changsha Station.

[6. Somehow, the periods of peak pollution are similar over the years (early and late part of January) with a bi/tri-weekly separation between them. Is there any specific reason for this?]

**Response 10:** Thanks for referee's suggestion. A biweekly separation between the periods of peak pollution in the THB could be resulted from the oscillation of cold air invasion in CEC. The atmospheric quasi-biweekly oscillation provides favorable conditions for the persistence of air pollution over the BTH region in winter. During the heavy PM<sub>2.5</sub> pollution events, the quasi-biweekly southerly anomalies prevail persistently over eastern China (Gao et al.,2020).

*[7. In section 3, local conditions leading to high pollution are mentioned. Are these not meteorological conditions? Perhaps, it may be mentioned as local and regional or large-scale meteorology.]*

**Response 11:** In the revised manuscript, it has been corrected with “Under stagnant meteorological conditions with local weak winds, strong and thick temperature inversion layers, sinking motion and low mixing layer heights are unfavourable for the diffusion of air pollutants for the formation of heavy air pollution.”

*[8. In line 215, there is a mention of the use of data from 31 urban monitoring stations. It will be better if a table is provided with all datasets used in the study with their source, frequency, and time periods.]*

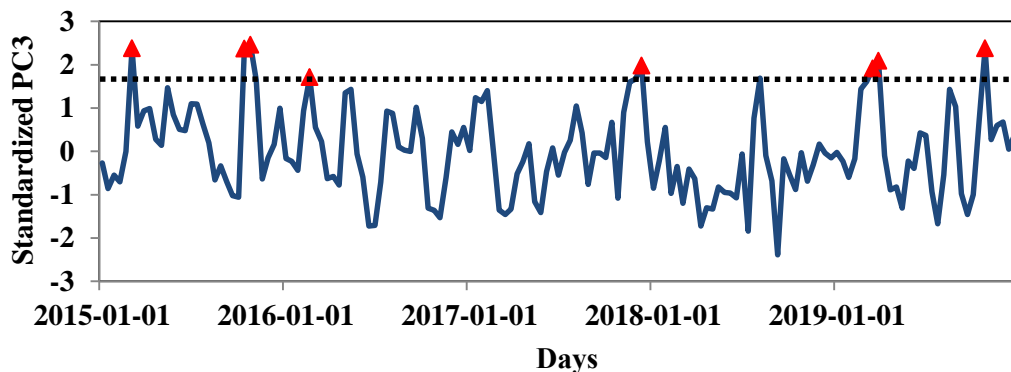
**Response 12:** In the revised manuscript, we have provided all datasets used in the study with their source, frequency, and time periods.

*[9. In Figure 2b, how much of the variance is explained by the mode shown?]*

**Response 13:** In the revised section 3.1 Analysis of modal results of MV-EOF decomposition, we have estimated the variance contribution rates of the first three modes 28.2%, 16.0%, and 12.0%, respectively, and the cumulative variance reaches 56.2%, all of which have passed the North test, indicating that the first three modes are independent of each other and can be clearly distinguished from other modes.

*[10. Selection of peak pollution events along with the time coefficient must be shown in figure 2 to identify the events.]*

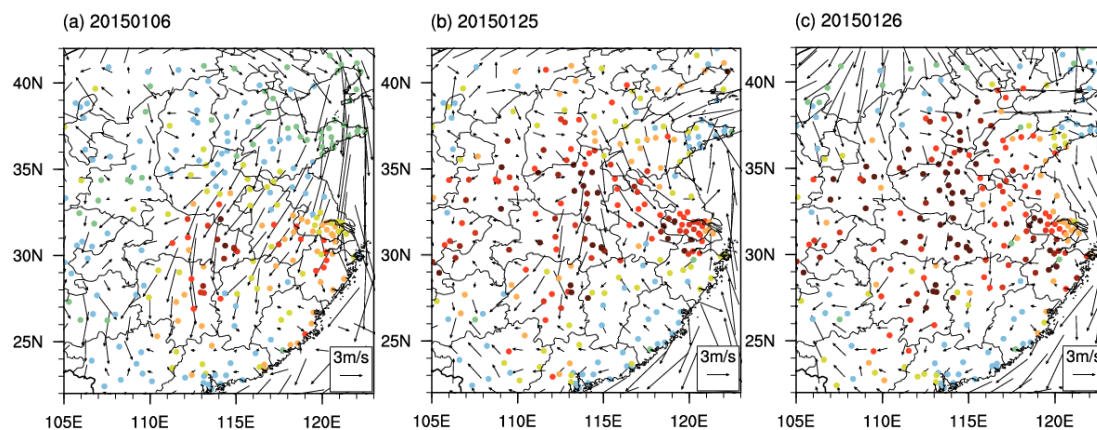
**Response 14:** Following the referee’s suggestion, we have added the new Fig. 6 to identify the typical events.



**Figure 6.** Daily changes of the standardized third-mode time coefficients PC3 in the THB in January of 2015-2019 with the red triangles representing the 8 peak pollution days with regional PM<sub>2.5</sub> transport selected based on the standardized PC3 exceeding 1.7 (black dot line) .

*[11. Since the peak episodes are few in number, is it possible to show each of the episodes for their PM<sub>2.5</sub> spatial patterns along with the circulation patterns (as sub-panels)? This will allow us to know whether the patterns are similar or dissimilar for each episode.]*

**Response 15:** Following the referee’s suggestion, Figure S1 showed the spatial distributions of PM<sub>2.5</sub> concentration and 10-m wind field at the 8 peak pollution days with regional PM<sub>2.5</sub> transport over CEC.



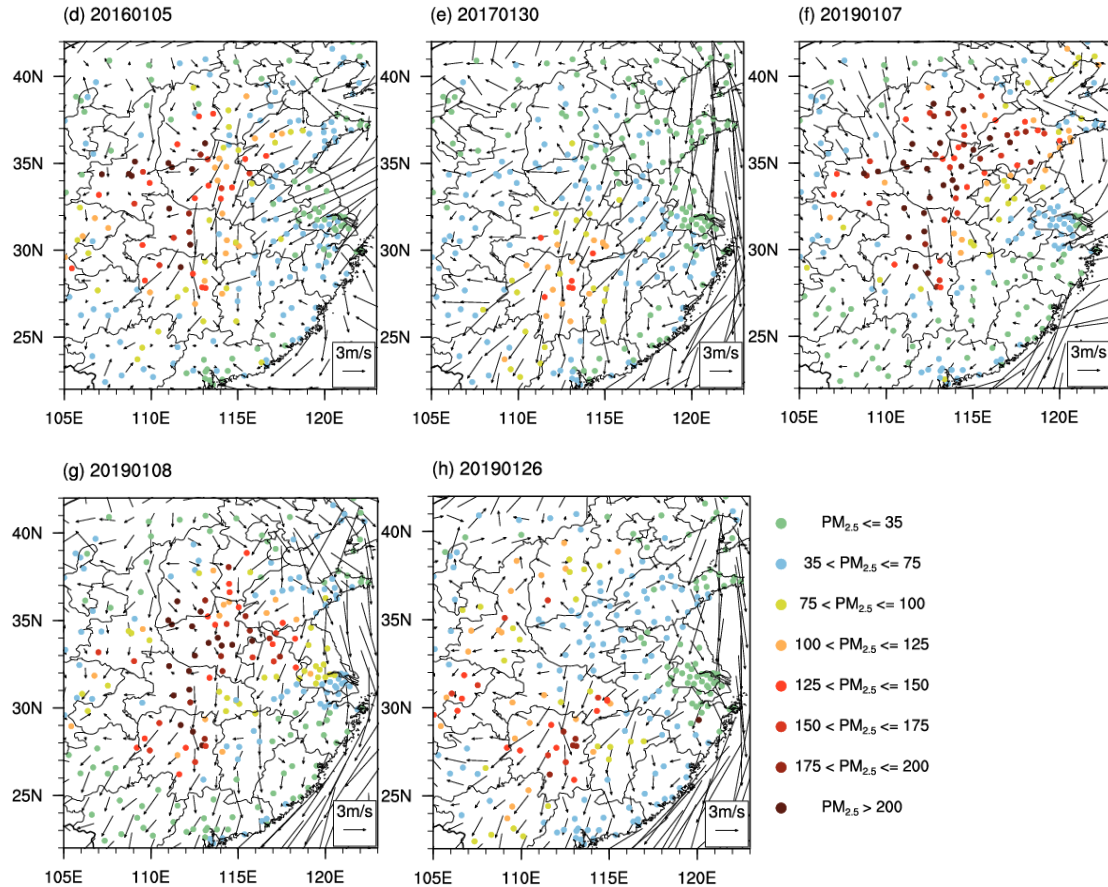


**Figure S1.** Spatial distribution of daily mean  $\text{PM}_{2.5}$  concentrations (unit:  $\mu\text{g m}^{-3}$ ) and 10m wind vectors (unit:  $\text{m s}^{-1}$ ) in central and eastern China (CEC) at 8 typical regional  $\text{PM}_{2.5}$  transport days in the THB, which is roughly outlined with the black lines.

[12. Use similar color bars and arrow lengths (Fig.3) so that comparison becomes easier.]

**Response 16:** In the revised manuscript, we have redrawn the Figures with similar color bars and same arrow lengths.

[13. Figure 4 corresponds to nationwide station data or reanalysis?]



**Response 17:** The revised Figure 8 (Figure 4 of the previous version) corresponded to nationwide station data.

[14. If showing from reanalysis, anomalies with respect the climatology will show a better pattern with slowing winds/lower or higher temperature over the large domain. It appears 4a corresponds to actual winds and 4b corresponds to anomalies in temp or are both anomalies.]

**Response 18:** The Figure 8 (Figure 4 in the previous version) corresponded to nationwide station data.

[ 15. In Fig. 8, it is seen that the topographic features are avoided to a large extent. However, will the 1000 Mb level correspond to the surface? If possible, the temperature below the surface should be avoided when showing such plots.]

**Response 19:** In the revised manuscript, we have accordingly modified the Figure as followings:

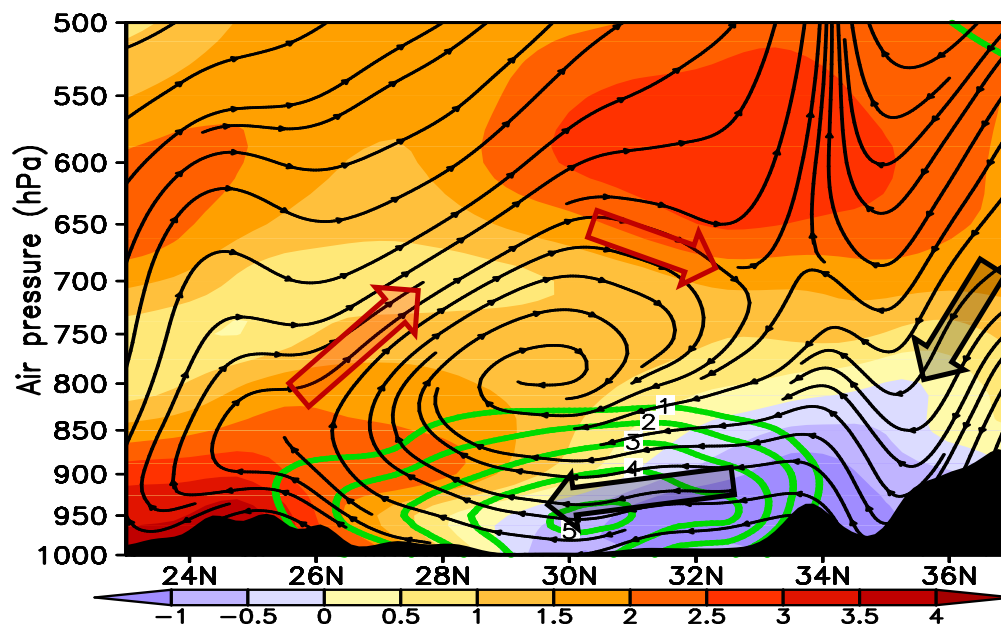


**Figure 10.** The meridional vertical cross-section (averaged over 112.25°E -113°E) of wind streamlines with vertical components multiplied by 10, anomalies of air



temperature (color contours, unit: °C) and wind speed (green contour lines, unit: m s<sup>-1</sup>). The wind streamlines are averaged for 8 days of transport-type PM<sub>2.5</sub> heavy pollution (Table 1) and the anomalies of air temperature and wind speed are calculated with the differences between the 8-day averages of transport-type PM<sub>2.5</sub> heavy pollution (Table 1) and the monthly mean in January of 2015-2019 based on the ERA-Interim daily data, and the THB topography is marked with the black shadow.

[ 16. Figure 9, sounding profiles could be shown along with climatology or the difference with respect to climatology similar to Fig. 10. This will clearly show the features during the pollution episodes. This will also validate/provide confidence in the reanalysis in case of any bias.]

**Response 20:** Following the referee’s suggestion, we have modified the Figure as follows:

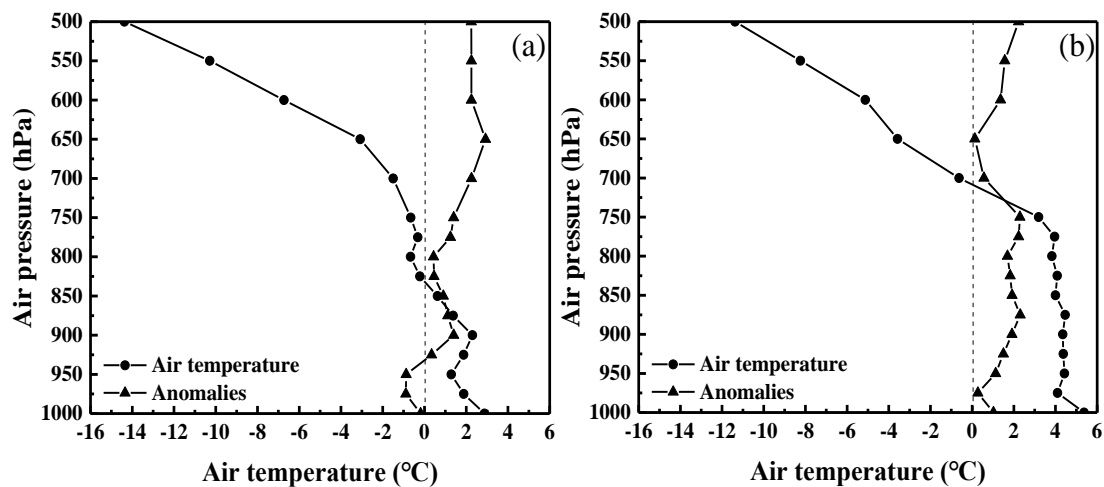


**Figure 11.** Vertical profiles of air temperature (dot lines) and anomalies (triangle lines) from sounding radiosonde observations at (a) Wuhan Station and (b) Changsha Station. All the profiles are averaged for 8 days of transport-type PM<sub>2.5</sub> peak pollution (Table 1) with the anomalies relative to the monthly mean in January of 2015-2019.

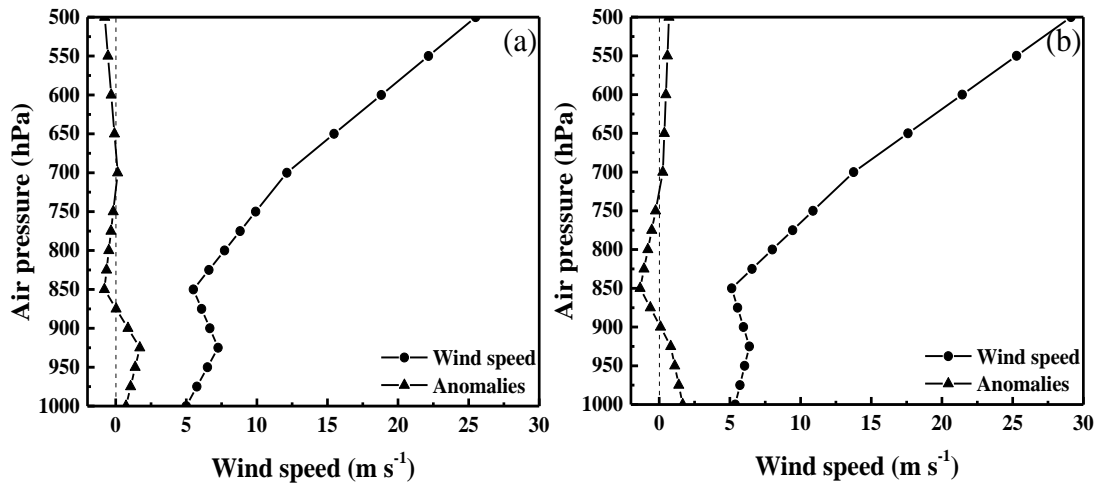


**Figure S3.** Vertical profiles of wind speed (dot lines) and anomalies (triangle lines) from sounding radiosonde observations at (a) Wuhan Station and (b) Changsha Station. All the profiles are averaged for 8 days of transport-type PM<sub>2.5</sub> peak pollution (Table 1) with the anomalies relative to the monthly mean in January of 2015-2019.

[ 17. Section 5 appears to me as an avoidable addition to the overall flow of the manuscript. Even removing this section may not affect the overall discussion of the paper.]

**Response 21:** Following the referee’s suggestion, we have removed this section in the revised manuscript.

[ 18. Section 5.2 details about WRF-Chem could be included in the data section.]

**Response 22:** We have removed this sections about WRF-Chem in the revised manuscript.

[ 19. Figures 8 and 13 could have a similar latitudinal spread so that the simulation could be compared with reanalysis easily. The simulations don’t compare with

*reanalysis according to this figure (perhaps, due to the different time periods, but could be checked with the exact period)]*

**Response 23:** In the revised manuscript, we deleted the figures following the referee's comments.

*[20. I find that the manuscript is most China-centric with no reference to the many important and interesting similar studies carried out elsewhere. This could be included in the future for completeness.]*

**Response 24:** Many thanks for referee's comments. In the revised manuscript, we have accordingly taken other international studies with literature cited in the paper into account as follows:

Regional transport of air pollutants is an important issue in atmospheric environment (Mayer, 1999; Jacobson, 2001; Kim et al., 2015; Singh et al., 2017; Crippa et al., 2018). Air pollution has become a public concern on atmospheric environment (Zhao et al., 2013; Chowdhury et al., 2018, 2019; Kanawade et al., 2019). The synoptic circulations exert an important impact on air pollutant transport (Hegarty et al., 2007; Demuzere et al., 2009; Russo et al., 2014; Pope et al., 2015; Bei et al., 2016; Yue et al., 2016). Biomass burning over the source region (i.e., northern Indochina) coincided with weak westerly system over the northern South China Sea, and the aerosols were transported to downwind regions by a cold front and low-level jet (LLJ) (Huang et al., 2020b). Exports of air pollutants from the North American boundary were the result of eastward advection over the ocean and transport in a weak warm conveyor belt airflow (Owen et al., 2006). The transport of air pollutants under the control of cold front system has a significant effect on air quality (Fuelberg et al., 2007; Xu et al., 2016b; Kang et al., 2019). Good air quality often occurs under cyclonic conditions, while poor air quality is frequently associated with anticyclonic conditions (Russo et al., 2014; Pope et al., 2015; Santurtún et al., 2015). The long-range transport of polluted air

masses from the North China Plain is the main factor for the sharp increases of PM<sub>2.5</sub> concentrations in central China (Lu et al., 2017, 2019b; Li et al., 2019b). Fine particulates can be regionally transported over a long distance with obvious trans-boundary transport, exerting an important effect on air pollution (Kim et al., 2012; Khuzestani et al., 2017; Li et al., 2019c; Yuan et al., 2019).